J Appl Electrochem (2008) 38:1553–1559
DOI 10.1007/s10800-008-9603-6

ORIGINAL PAPER

# Electrochemical and theoretical studies of thienyl-substituted amino triazoles on corrosion inhibition of copper in 0.5 M $H_2SO_4$

**Yong-Ming Tang · Yun Chen · Wen-Zhong Yang · Ying Liu · Xiao-Shuang Yin · Jin-Tang Wang**

Received: 22 January 2008 / Accepted: 15 May 2008 / Published online: 31 May 2008


**Abstract** 2,5-Bis(2-thienyl)-4-amino-1,2,4-triazole (2-TAT) and 2,5-bis(3-thienyl)-4-amino-1,2,4-triazole (3-TAT) have been studied as inhibitors for the corrosion of copper in 0.5 M $H_2SO_4$ using potentiodynamic polarization and electrochemical impedance spectroscopy (EIS). The inhibition efficiency of the triazole compounds increases with increasing concentration, and the effect of 3-TAT is better than that of 2-TAT with the same concentration. Potentiodynamic polarization measurements indicate the triazole compounds act as mixed type inhibitors in 0.5 M $H_2SO_4$. The adsorption of the triazole compounds is found to obey the Langmuir adsorption isotherm. High significant correlations for the triazole compounds are obtained between inhibition efficiency and quantum chemical parameters ($R = 0.975$) using the quantitative structure–activity relationship (QSAR) method.

**Keywords** Triazole · Corrosion inhibitor · Adsorption · Quantitative structure–activity relationship · PM3

## 1 Introduction

Due to its excellent thermal conductivity and good mechanical workability copper is widely used in heating and cooling systems [1]. In order to maintain thermal efficiency, periodic cleaning in sulfuric acid (or hydrochloric acid) pickling solutions for the removal of scale and corrosion products is necessary [2]. In many cases, corrosion inhibitors can be used to prevent copper corrosion in acidic solution.

Many organic compounds, specially containing polar groups and/or substituted heterocycle including nitrogen, sulfur, and oxygen in their structures [3–9], have been reported to inhibit copper corrosion. The inhibiting action of these organic compounds is usually attributed to their interaction with the copper surface via adsorption [2], and to their molecular structure [10]. The molecular structure, including the electronic parameters, can be obtained by means of theoretical calculations by using the computational methodologies of quantum-chemistry [10, 11]. Quantum chemical calculation has been used recently to explain the mechanism of corrosion inhibition [12–14], and has proved to be a very powerful tool for studying the mechanism [15–17].

In this work, the effects of two isomers of thienyl-substituted amino triazoles, namely 2,5-bis(2-thienyl)-4-amino-1,2,4-triazole (2-TAT) and 2,5-bis(3-thienyl)-4-amino-1,2,4-triazole (3-TAT) (Scheme 1), on inhibition properties on the corrosion of copper in 0.5 M $H_2SO_4$ have been studied. Potentiodynamic polarization and electrochemical impedance spectroscopy (EIS) were used. Also the relationship between calculated quantum chemical parameters and experimental inhibition efficiencies of the inhibitors was discussed.

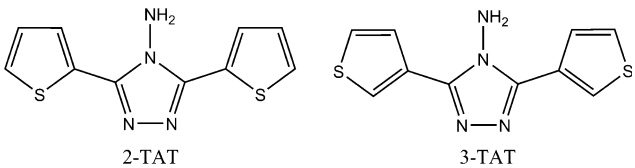


**Scheme 1** Structures of 2-TAT and 3-TAT

Y.-M. Tang (✉) · Y. Chen · W.-Z. Yang · Y. Liu · X.-S. Yin · J.-T. Wang
College of Science, Nanjing University of Technology, Nanjing 210009, People's Republic of China
e-mail: tangym@njut.edu.cn

## 2 Materials and methods

The copper electrode was made from 99.9% pure copper rods. The rod specimen was embedded in a Teflon holder using epoxy resin with an exposed area of 0.21 $cm^2$. Before each experiment the electrode was first mechanically polished with various grades of sandpaper (up to 1200 grit) and then ultrasonically cleaned in acetone for 2 min, followed by a rinse in double-distilled water.

Regent-grade $H_2SO_4$ was used, and the aggressive solution was made up with double-distilled water. 2-TAT and 3-TAT were synthesized in the laboratory following the procedure reported previously [18].

A traditional three-electrode cell was used for electrochemical measurements. A platinum sheet electrode was used for the auxiliary electrode, and the reference electrode was a saturated calomel electrode (SCE) with a Luggin capillary. All potentials were measured with respect to the SCE.

Electrochemical experiments were performed using a ZAHNER IM6ex electrochemical workstation. For potentiodynamic polarization experiments, the potential was scanned at a scan rate of 0.2 mV $s^{-1}$. The electrochemical impedance spectroscopy (EIS) experiments were performed at open-circuit potential over a frequency range of 0.01 Hz–100 kHz. The sinusoidal potential perturbation was 5 mV in amplitude. Electrochemical data were analyzed by a ZAHNER THALES software.

All theoretical computations were carried out using a semi-empirical PM3 method from the program package MOPAC2007. A full optimization of all geometrical variables without any symmetry constraint was performed at the Restricted Hartree-Fock (RHF) level. Molecular structures were optimized to a gradient <0.01 in the vacuum phase. The following quantum chemical indices were considered: the energy of the highest occupied molecular orbital ($E_{HOMO}$), the energy of the lowest unoccupied molecular orbital ($E_{LUMO}$), $\Delta E = E_{HOMO} - E_{LUMO}$ and the dipole moment ($\mu$).

## 3 Results and discussion

### 3.1 Potentiodynamic polarization

Anodic and cathodic polarization curves for copper in 0.5 M $H_2SO_4$ with various concentrations of 2-TAT (from 0.5 to 6.0 mM) and 3-TAT (from 0.25 to 2.0 mM) are shown in Figs. 1 and 2, respectively. The presence of different concentrations of 2-TAT and 3-TAT reduce the anodic and cathodic current densities, and the suppression in current increases as the inhibitor concentration increases; this indicates the inhibiting effects of the two triazole

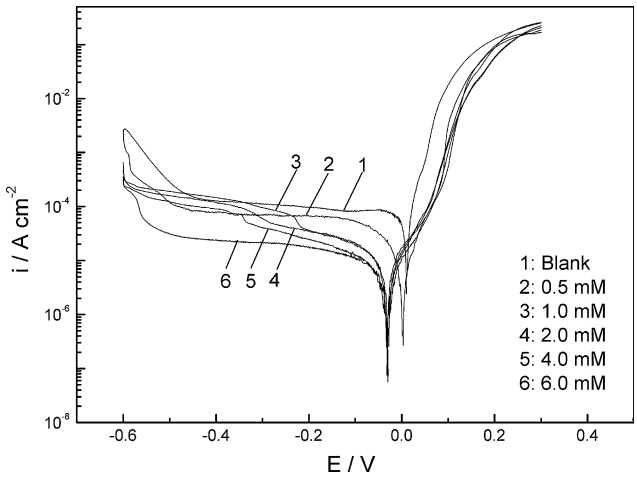


**Fig. 1** Polarization curves for copper in 0.5 M $H_2SO_4$ containing various concentrations of 2-TAT at 30 °C

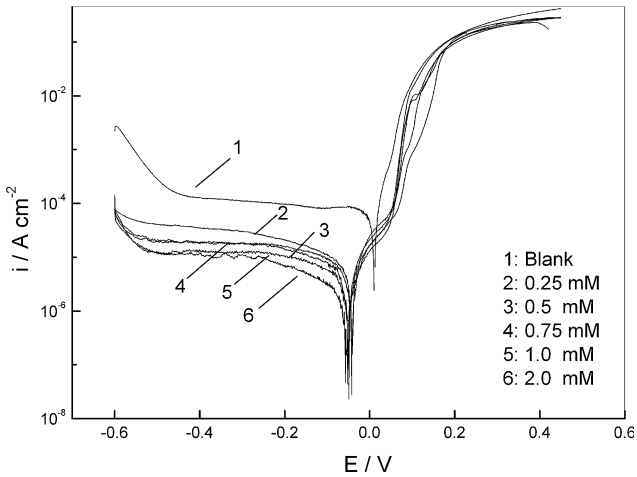


**Fig. 2** Polarization curves for copper in 0.5 M $H_2SO_4$ containing various concentrations of 3-TAT at 30 °C

compounds. The anodic polarization curve displays Tafelian linearity in the free-inhibitor solution. However, in the presence of inhibitors, at potentials of about 0.09 V for 2-TAT and 0.13 V for 3-TAT a sharp increase in anodic current is observed. This effect can be interpreted as follows: the triazoles, like other adsorption inhibitors, should adsorb at the metal-solution interface at potentials close to the corrosion potential [19], but at higher potentials, such as about 0.09 V for 2-TAT and 0.13 V for 3-TAT, significant dissolution of the copper surface would lead to desorption of the adsorbed triazole compounds from the electrode surface [20]. In this case, the desorption rate of triazole compounds is higher than their adsorption rate [21].

Electrochemical kinetic parameters, i.e., corrosion potential ($E_{corr}$), cathodic and anodic Tafel slope ($b_c$ and $b_a$) and corrosion current density ($i_{corr}$), obtained by extrapolation of the Tafel lines, are presented in Table 1.

**Table 1** Electrochemical parameters for copper in 0.5 M $H_2SO_4$ containing various concentrations of inhibitors at 30 °C

| | $C_{inh}$ (mM) | $E_{corr}$ (mV) | $i_{corr}$ (μA $cm^{-2}$) | $b_c$ (Mv $dec^{-1}$) | $b_a$ (Mv $dec^{-1}$) | $E$ (%) |
|---|---|---|---|---|---|---|
| Blank | | +16 | 3.60 | −1660 | 32 | – |
| 2-TAT | 0.5 | 0 | 1.44 | −490 | 66 | 60.0 |
| | 1.0 | −21 | 0.81 | −631 | 65 | 77.6 |
| | 2.0 | −24 | 0.67 | −469 | 61 | 81.4 |
| | 4.0 | −25 | 0.41 | −575 | 68 | 88.6 |
| | 6.0 | −20 | 0.35 | −305 | 64 | 90.3 |
| 3-TAT | 0.25 | −21 | 0.62 | −614 | 84 | 81.2 |
| | 0.50 | −12 | 0.53 | −400 | 88 | 84.0 |
| | 0.75 | −35 | 0.38 | −369 | 84 | 88.4 |
| | 1.0 | −26 | 0.27 | −339 | 83 | 92.5 |
| | 2.0 | −36 | 0.23 | −333 | 89 | 93.6 |

The inhibition efficiencies ($E\%$) of the triazole compounds in 0.5 M $H_2SO_4$ are also given in Table 1. The inhibition efficiency is defined as:

$$E\% = \frac{i^0_{corr} - i_{corr}}{i^0_{corr}} \times 100 \quad (1)$$

where $i^0_{corr}$ and $i_{corr}$ are the corrosion current density values without and with inhibitor, respectively.

The slight shifts of $E_{corr}$ values towards negative direction are found in the presence of various concentrations of the triazole compounds in 0.5 M $H_2SO_4$. Generally, increase in inhibitor concentration shifts corrosion potential negatively. This can be explained by a small domination of the cathodic reaction inhibition [1]. However, the triazoles influence the anodic reaction at potentials greater than the desorption potential (Figs. 1, 2). This indicates that 2-TAT and 3-TAT exhibit both cathodic and anodic inhibition effects. Small changes in potentials can be a result of the competition of the anodic and the cathodic inhibiting reactions, and of the metal surface condition [1]. Meanwhile, from Table 1, the slopes of the cathodic Tafel lines ($b_c$) and anodic Tafel lines ($b_a$) are observed to change with addition of triazole compounds, which indicates influence on both the cathodic and anodic reactions; the cathodic curves are more affected. Thus 2-TAT and 3-TAT act as mixed type inhibitors for copper in 0.5 M $H_2SO_4$.

Inhibition efficiency ($E\%$) increases with increasing concentration in 0.5 M $H_2SO_4$. But with the same concentration the corrosion inhibition ability of 3-TAT is better than that of 2-TAT. With a dosage of 1 mM, for instance, the inhibition efficiency of 3-TAT exceeds 90%, while that of 2-TAT is merely 77.6%.

### 3.2 Effect of temperature

In order to investigate the effect of temperature potentiodynamic polarization for copper weas carried out at different temperature (25–40 °C) in the absence and presence of 2 mM of inhibitor. Electrochemical parameters and inhibition efficiencies are given in Table 2. The corrosion current density increases with increasing temperature, both in uninhibited and inhibited solutions. Small changes in inhibition efficiencies are observed in the range of temperature studied.

Corrosion reaction can be regarded as Arrhenius-type processes; consequently, the activation parameters can be calculated using theArrhenius equation:

$$i_{corr} = k \exp\left(-\frac{E_a}{RT}\right) \quad (2)$$

where $k$ is the pre-exponential factor, and $E_a$ is the activation energy of the corrosion process. Figure 3 presents the Arrhenius plots of the natural logarithm of the corrosion current density vs. 1/T for copper in 0.5 M $H_2SO_4$ without and with addition of 2-TAT and 3-TAT. The calculated values of activation energy are given in Table 3. It is clear that the activation energy values obtained in the presence of inhibitors are higher than that obtained in the absence of inhibitor, indicating that the addition of inhibitors enhances corrosion resistance of. The increase in activation energy value in the presence of 2-TAT is less than for 3-TAT, which may be attributed to the consumption of some energy in the adsorption process of 2-TAT [22–24].

### 3.3 Electrochemical impedance spectroscope (EIS)

The corrosion of copper in 0.5 M $H_2SO_4$ in the presence of the triazole compounds was investigated by the EIS method at 30 °C after 2 h immersion. Nyquist plots in the absence and presence of the triazole compounds are presented in Figs. 4 and 5. It is apparent that all Nyquist plots show a single capacitive loop, both in uninhibited and inhibited solutions. The impedance data of copper in 0.5 M $H_2SO_4$ are analyzed using the circuit in Fig. 6, in which $R_s$

**Table 2** Electrochemical parameters for copper in 0.5 M $H_2SO_4$ and 0.5 M $H_2SO_4$ + 2 mM inhibitors at different temperature

| Temp. (°C) | Blank | | 2-TAT | | | 3-TAT | | |
|---|---|---|---|---|---|---|---|---|
| | $E_{corr}$ (mV) | $i_{corr}$ (μA cm$^{-2}$) | $E_{corr}$ (mV) | $i_{corr}$ (μA cm$^{-2}$) | $E$ (%) | $E_{corr}$ (mV) | $i_{corr}$ (μA cm$^{-2}$) | $E$ (%) |
| 25 | −11 | 2.66 | −34 | 0.45 | 83.1 | −24 | 0.14 | 94.7 |
| 30 | +16 | 3.60 | +3 | 0.67 | 81.4 | −36 | 0.23 | 93.6 |
| 35 | −3 | 5.35 | +26 | 0.91 | 83.0 | −68 | 0.48 | 91.0 |
| 40 | −44 | 5.81 | −106 | 1.17 | 80.0 | +18 | 0.71 | 92.0 |

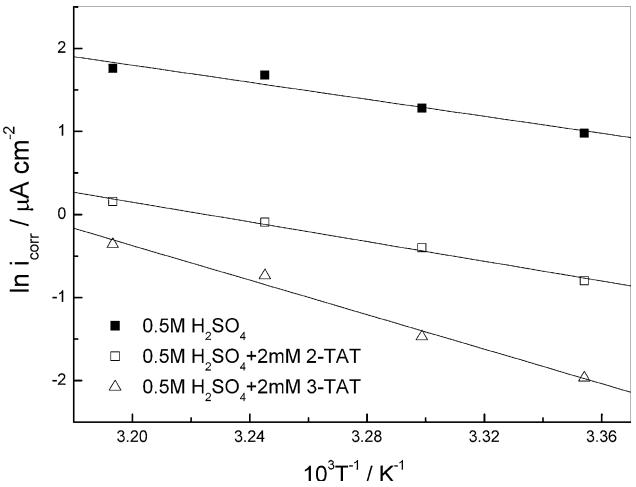


**Fig. 3** Arrhenius plots for copper in 0.5 M $H_2SO_4$ and 0.5 M $H_2SO_4$ + 2 mM inhibitors

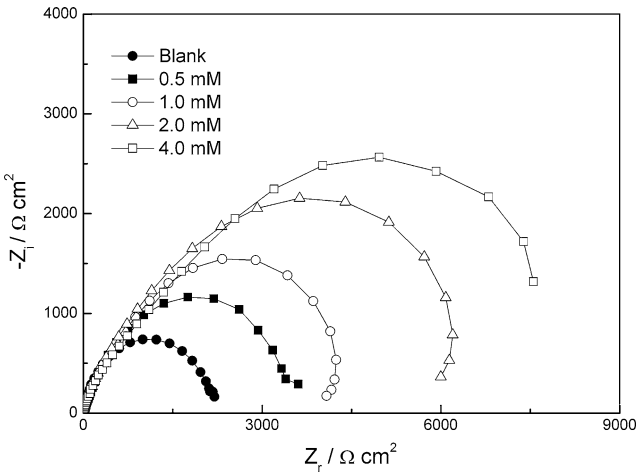


**Fig. 4** Nyquist plots for copper in 0.5 M $H_2SO_4$ containing different concentrations of 2-TAT

**Table 3** Activation energy for the corrosion of copper in 0.5 M $H_2SO_4$ without and with the addition of 2 mM inhibitors

| | $E_a$ (kJ mol$^{-1}$) |
|---|---|
| Blank | 45.7 |
| 2-TAT | 46.3 |
| 3-TAT | 86.4 |

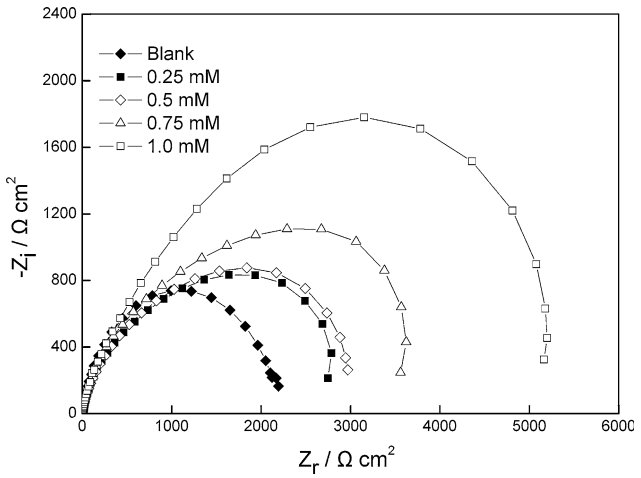


**Fig. 5** Nyquist plots for copper in 0.5 M $H_2SO_4$ containing different concentrations of 3-TAT

represents the electrolyte resistance, $R_t$ the charge transfer resistance. One constant phase element ($Q_{dl}$) is substituted for the capacitive element to give a more accurate fit, as most capacitive loops are depressed semi-circles rather than regular semi-circles [25]. The impedance of a constant phase element is described by the expression:

$$Z_Q = Y_0^{-1}(j\omega)^{-n} \quad (3)$$

where $Y_0$ is a proportional factor, $n$ has the meaning of a phase shift. According to Mansfeld et al. [26], the values of the double layer capacitance ($C_{dl}$) can be obtained from the equation:

$$C_{dl} = Y_0(\omega''_m)^{n-1} \quad (4)$$

where $\omega''_m$ is the frequency at which the imaginary part of the impedance has a maximum. Values of elements fitted and that of $C_{dl}$ calculated are listed in Table 4.

**Fig. 6** Equivalent circuits used to fit the impedance spectrum of copper

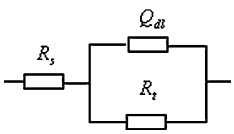


It can be seen from Table 4 that the values of charge transfer resistance increase with inhibitor concentration [22]. In the case of impedance studies, $E\%$ is calculated from the equation:

**Table 4** Fitting the EIS for copper in 0.5 M $H_2SO_4$ containing different concentrations of inhibitors by the circuit shown in Fig. 6

| | $C_{inh}$ (mM) | $R_s$ ($\Omega$ cm$^2$) | $R_t$ (k$\Omega$ cm$^2$) | $C_{dl}$ ($\mu$F cm$^{-2}$) | $E$ (%) |
|---|---|---|---|---|---|
| Blank | | 0.3 | 2.2 | 1262.2 | – |
| 2-TAT | 0.5 | 0.2 | 3.4 | 260.4 | 35.3 |
| | 1.0 | 0.2 | 4.8 | 222.4 | 55.3 |
| | 2.0 | 0.3 | 7.2 | 209.0 | 70.0 |
| | 4.0 | 0.1 | 9.3 | 201.0 | 76.8 |
| 3-TAT | 0.25 | 0.3 | 3.3 | 511.4 | 33.8 |
| | 0.50 | 0.2 | 3.5 | 471.8 | 39.0 |
| | 0.75 | 0.3 | 4.4 | 361.6 | 51.0 |
| | 1.0 | 0.2 | 5.9 | 195.0 | 63.6 |

$$E\% = \frac{R_t' - R_t}{R_t'} \times 100 \quad (5)$$

where $R_t$ and $R_t'$ are the values of the charge transfer resistance without and with inhibitor, respectively. $E\%$ increases with inhibitor concentration in the presence of both 2-TAT and 3-TAT, and the inhibition efficiency of 3-TAT is higher than that of 2-TAT with the same concentration. The impedance study also confirms the inhibiting characters of 2-TAT and 3-TAT obtained with potentiodynamic polarization. It is also noticed that the $C_{dl}$ values tend to decrease when the concentration of the triazole compounds increases. This decrease in $C_{dl}$, which can result from a decrease in local dielectric constant and/or an increase in the thickness of the electrical double layer, suggests that the triazole molecules function by adsorption at the metal/solution interface [27].

### 3.4 Adsorption isotherm

Basic information on the interaction between the inhibitor and the metal surface can be provided by the adsorption isotherm [27], which depends on the degree of electrode surface coverage ($\theta$). The EIS data were used to evaluate the surface coverage values as follows [28]:

$$\theta = \frac{C_{dl(\theta=0)} - C_{dl,\theta}}{C_{dl(\theta=0)} - C_{dl(\theta=1)}} \quad (6)$$

where $C_{dl(\theta=0)}$ and $C_{dl(\theta=1)}$ are the double layer capacitances of the inhibitor-free and entirely inhibitor-covered surfaces, respectively, $C_{dl,\theta}$ is the composite total double layer capacitance for any intermediate coverage $\theta$. The surface coverage values ($\theta$) were tested graphically to allow fitting of a suitable adsorption isotherm. The plots of $C_{inh}/\theta$ against $C_{inh}$ for 2-TAT and 3-TAT give straight lines with almost unit slope (Fig. 7), indicating that the triazole compounds obey the Langmuir adsorption isotherm in 0.5 M $H_2SO_4$

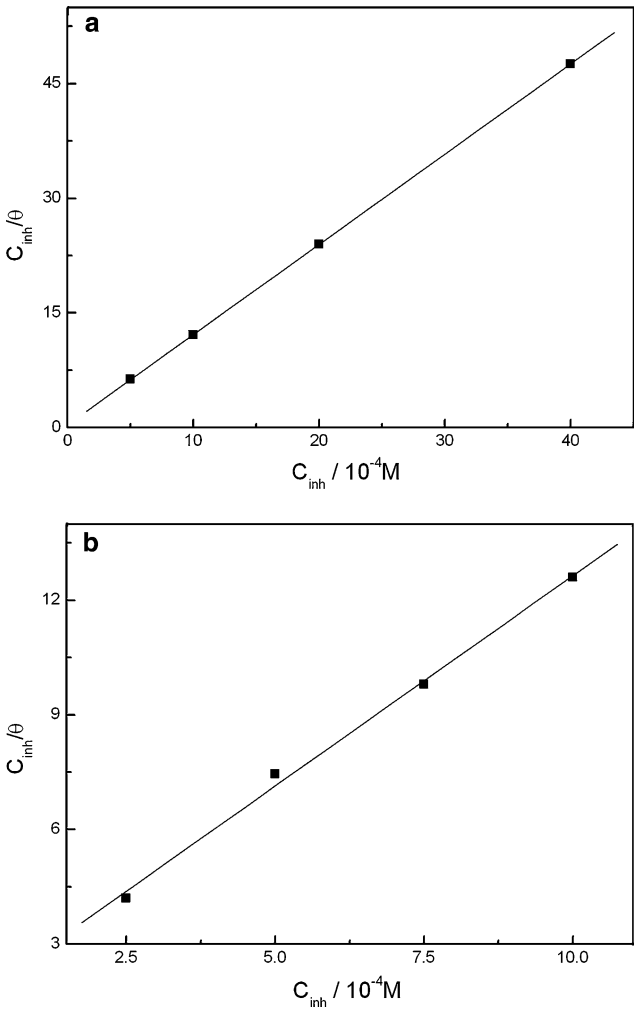


**Fig. 7** Langmuir adsorption plots for copper in 0.5 M $H_2SO_4$ containing different concentrations of 2-TAT (**a**) and 3-TAT (**b**) from capacitance values

$$\theta = \frac{KC_{inh}}{1 + KC_{inh}} \quad (7)$$

where $K$ is the equilibrium constant of the adsorption process. The free energy of adsorption $\Delta G_{ads}$ can be calculated from the equation:

$$K = \frac{1}{55.5}\exp\left(\frac{-\Delta G_{ads}}{RT}\right) \quad (8)$$

The values of $\Delta G_{ads}$ were calculated to $-35.8$ and $-38.1$ kJ mol$^{-1}$ of 2-TAT and 3-TAT, respectively. The large negative values of $\Delta G_{ads}$ reveal that the adsorption process takes place spontaneously and the adsorbed layer on the surface of copper is highly stable [28]. Moreover, the higher absolute value of $\Delta G_{ads}$ obtained for 3-TAT indicates that the latter is more strongly adsorbed on the copper surface in 0.5 M $H_2SO_4$. The result is agreement with that obtained from electrochemical techniques.

**Table 5** Calculated quantum chemical parameters of the triazole compounds

| Molecule | $E_{HOMO}$ (eV) | $E_{LUMO}$ (eV) | $\mu_D$ (Debye) | $\Delta E$ (eV) |
|---|---|---|---|---|
| 2-TAT | −9.06 | −1.22 | 5.021 | −7.84 |
| 3-TAT | −8.94 | −0.96 | 5.159 | −7.98 |

It is well known that values of $\Delta G_{ads}$ of the order of 20 kJ $mol^{-1}$ or lower indicate physisorption; those of the order of 40 kJ $mol^{-1}$ or higher involve charge sharing or a transfer from the inhibitor molecules to the metal surface to form a co-ordinate type of bond [29, 30]. Accordingly, the values of $\Delta G_{ads}$ obtained in the present study indicate that 2-TAT and 3-TAT in 0.5 M $H_2SO_4$ adsorb on the copper by a chemisorption-based mechanism.

### 3.5 Theoretical computation

Quantitative structure–activity relationship (QSAR) was used to study the effect of molecular structure on the inhibition efficiency of the two triazole inhibitors. Table 5 shows the quantum chemical calculation parameters ($E_{HOMO}$, $E_{LUMO}$ and $\mu$) obtained by the semi-empirical PM3 method, and the energy band gap $\Delta E(=E_{HOMO} - E_{LUMO})$ is also listed. $E_{HOMO}$ is often associated with the electron donating ability of a molecule. High $E_{HOMO}$ values indicate that the molecule has a tendency to donate electrons to appropriate acceptor molecules with low energy empty molecular orbital. Increasing values of the $E_{HOMO}$ facilitate adsorption (and therefore inhibition) by influencing the transport process through the adsorbed layer [31–33]. $E_{LUMO}$ indicates the ability of the molecules to accept electrons. The lower value of $E_{LUMO}$, the more probable it is that the molecule would accept electrons [31–33]. Low absolute values of the energy band gap ($\Delta E$) gives good inhibition efficiencies, because the energy to remove an electron from the last occupied orbital will be low [34]. For the dipole moment ($\mu$), higher values will favorite enhancement of corrosion inhibition [35].

It is clear from Table 5 that small difference between the values obtained for the $E_{HOMO}$ and $E_{LUMO}$ corresponding to both isomers is observed (0.12 eV for difference of $E_{HOMO}$ and 0.26 eV for difference of $E_{LUMO}$). This indicates a very similar capacity for charge donation and acceptance to the metallic surface [28]. Concerning the values of the dipole moment $\mu$ and the energy band gap $\Delta E$, no direct correlation can be obtained with inhibition efficiencies. However, an important difference can be observed in the location of the HOMO density (Fig. 8). For 2-TAT the HOMO density is located relative equally on triazole ring and thiophene rings, whereas for 3-TAT the HOMO density on thiophene rings is higher than that on the triazole ring.

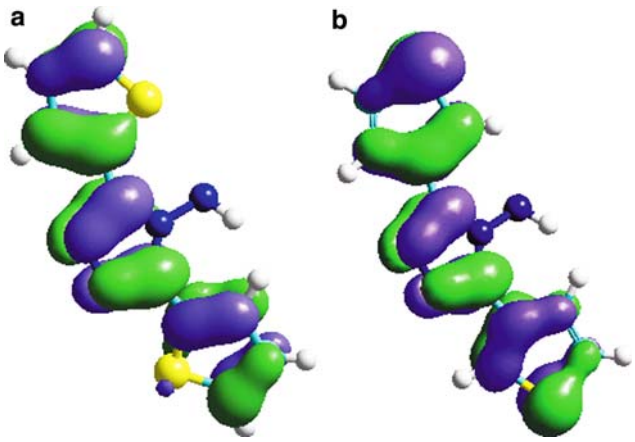


**Fig. 8** Localization of the HOMO orbitals of 2-TAT (**a**) and 3-TAT (**b**)

Since individual quantum chemical parameters cannot explain the differences observed in inhibition efficiencies of the triazole compounds, there may be a composite index of more than one parameter, which might affect the efficiency [28]. Accordingly, quantum chemical parameters for inhibitors were correlated with their experimental inhibition efficiencies using regression analysis. A non-linear model (LKP) proposed by Lukovits et al. [35, 36] for the interaction of corrosion inhibitors with metal surfaces in acidic solutions has been used in the present study according to the following equation [35, 37]:

$$E_i = \frac{(Ax_j + B)C_i}{1 + (Ax_j + B)C_i} \times 100 \tag{9}$$

where $E_i$ is the inhibition efficiency, $A$ and $B$ are the regression coefficients determined by regression analysis, $x_j$ is a quantum chemical index characteristic for the molecule ($j$) and $C_i$ denotes the concentration in an experiment $i$. In the present case, multiple regression analysis was performed, and $x_j$ is constructed as a composite index of quantum chemical parameters, $E_{HOMO}$, $E_{LUMO}$ and $\mu$. The following equation is obtained for the triazole compounds:

$$E_i = \frac{(7.60E_{HOMO} + 45.14E_{LUMO} + 15.56\mu + 46.52)C_i}{1 + (7.60E_{HOMO} + 45.14E_{LUMO} + 15.56\mu + 46.52)C_i} \times 100 \tag{10}$$

High significant multiple correlation coefficient ($R = 0.975$) between experimental inhibition efficiencies, $E_{exp}\%$, and calculated inhibition efficiencies, $E_{cal}\%$, is obtained as presented in Fig. 9. This result demonstrates that a link may exist between a composite index of some of quantum chemical parameters and the corrosion inhibition efficiency of a given molecule. Accordingly, these results

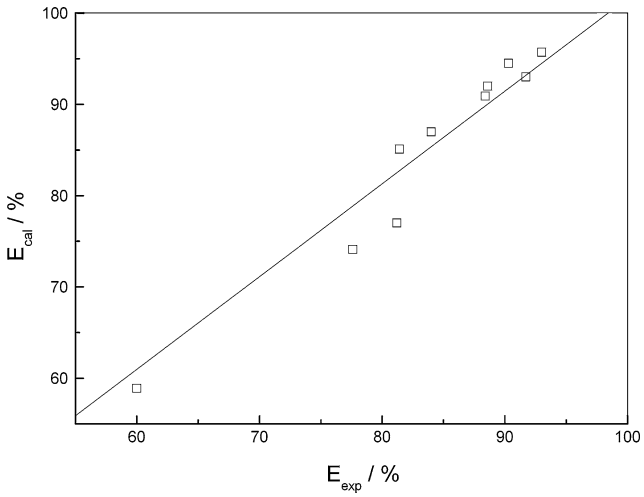


**Fig. 9** Correlation between the experimental and calculated inhibition efficiencies by the LKP model for the triazole compounds in 0.5 M $H_2SO_4$

might help in planning of new, effective inhibitor molecules [38].

## 4 Summary

2-TAT and 3-TAT are effective inhibitors of corrosion of copper exposed to 0.5 M $H_2SO_4$, and inhibition efficiency of 3-TAT is higher than that of 2-TAT with the same concentration. The concentration dependence of the inhibition efficiency calculated from polarization and EIS has the same tendency. Polarization measurements show that 2-TAT and 3-TAT are mixed-type inhibitors. Adsorption of 2-TAT and 3-TAT on the copper surface in 0.5 M $H_2SO_4$ obeys the Langmuir isotherm. Direct correlation, for 2-TAT and 3-TAT, between their molecular structure and inhibition efficiency has been established by using a non-linear model joining the inhibition efficiency to quantum chemical parameters ($E_{HOMO}$, $E_{LUMO}$ and $\mu$). A high significant multiple correlation coefficient ($R = 0.975$) between experimental and calculated inhibition efficiencies is obtained.

## References

1. Stupnišek-Lisac E, Gazivoda A, Madžarac M (2002) Electrochim Acta 47:4189
2. Sherif EM, Erasmus RM, Comins JD (2007) J Colloid Interface Sci 311:144
3. Elmorsi MA, Hassanien AM (1999) Corros Sci 41:2337
4. Abd El-Maksoud SA (2004) J Electroanal Chem 565:321
5. Sherif EM, Erasmus RM, Comins JD (2007) J Colloid Interface Sci 306:96
6. Quartarone G, Moretti G, Bellomi T, Capobianco G, Zingales A (1998) Corrosion 54:606
7. Christy AG, Lowe A, Otieno-Alego V, Stoll M, Webster RD (2004) J Appl Electrochem 34:225
8. Gomma GK (1998) Mater Chem Phys 56:27
9. Bastidas JM, Pinilla P, Cano E, Polo JL, Miguel S (2003) Corros Sci 45:427
10. Rodríguez-Valdez LM, Martínez-Villafañe A, Glossman-Mitnik D (2005) J Mol Struct (Theochem) 713:65
11. El Ashry ESH, El Nemr A, Essawy SA, Ragab S (2008) Prog Org Coat 61:11
12. El Ashry ESH, El Nemr A, Essawy SA, Ragab S (2006) Electrochim Acta 51:3957
13. Zhao P, Liang Q, Li Y (2005) Appl Surf Sci 252:1596
14. Xiao-Ci Y, Hong Z, Ming-Dao L, Hong-Xuan R, Lu-An Y (2000) Corros Sci 42:645
15. Wang D, Li S, Ying Y, Wang M, Xiao H, Chen Z (1999) Corros Sci 41:1911
16. Bereket G, Öğretir C, Hür E (2002) J Mol Struct (Theochem) 578:79
17. Öğretir C, Mihici B, Bereket G (1999) J Mol Struct (Theochem) 488:223
18. Bentiss F, Lagrenée M, Traisnel M, Mernari B, Elattari H (1999) J Heterocycl Chem 36:149
19. Quartarone G, Bellomi T, Zingales A (2003) Corros Sci 45:715
20. Drazic DM, Drazic VJ, Jevtic V (1989) Electrochim Acta 34:1251
21. El Mehdi B, Mernari B, Traisnel M, Bentiss F, Lagrenée M (2002) Mater Chem Phys 77:489
22. Larabi L, Benali O, Mekelleche SM, Harek Y (2006) Appl Surf Sci 253:1371
23. Szauer T, Brand A (1981) Electrochim Acta 26:1219
24. Oguzie EE, Onuoha GN, Onuchukwu AI (2005) Mater Chem Phys 89:305
25. Ma HY, Chen SH, Yin BS, Zhao SY, Liu XQ (2003) Corros Sci 45:867
26. Hsu CH, Mansfeld F (2001) Corrosion 57:747
27. Lagrenée M, Mernari B, Bouanis M, Traisnel M, Bentiss F (2002) Corros Sci 44:573
28. Lebrini M, Lagrenée M, Traisnel M, Gengembre L, Vezin H, Bentiss F (2007) Appl Surf Sci 253:9267
29. Donahue FM, Nobe K (1965) J Electrochem Soc 112:886
30. Kamis E, Belluci F, Latanision RM, El-Ashry ESH (1991) Corrosion 47:677
31. Ashassi-Sorkhabi H, Shaabani B, Seifzadeh D (2005) Electrochim Acta 50:3446
32. Ashassi-Sorkhabi H, Shaabani B, Seifzadeh D (2005) Appl Surf Sci 239:154
33. Özcan M, Dehri İ, Erbil M (2004) Appl Surf Sci 236:155
34. Moretti G, Guidi F, Grion G (2004) Corros Sci 46:387
35. Lukovits I, Pálfi K, Bakó I, Kálmán E (1997) Corrosion 53:915
36. Lukovits I, Bakó I, Shaban A, Kálmán E (1998) Electrochim Acta 43:131
37. Khaled KF, Babić-Samardžija K, Hackerman N (2005) Electrochim Acta 50:2515
38. Khalil N (2003) Electrochim Acta 48:2635